Article:
Hall, DA, Mori, T, Comyn, TP et al. (2 more authors) (2013) Residual stress relief due to fatigue in tetragonal lead zirconate titanate ceramics. Journal of Applied Physics, 114 (2). 024103. ISSN 0021-8979

https://doi.org/10.1063/1.4812326

Residual stress relief due to fatigue in tetragonal lead zirconate titanate ceramics

D. A. Hall,[1,a)] T. Mori,[1] T. P. Comyn,[2] E. Ringgaard,[3] and J. P. Wright[4]
[1]*School of Materials, University of Manchester, Grosvenor St., Manchester M1 7HS, United Kingdom*
[2]*Institute for Materials Research, Woodhouse Lane, University of Leeds, LS2 9JT, United Kingdom*
[3]*Meggitt Sensing Systems, Hejreskovvej 18A, 3490 Kvistgaard, Denmark*
[4]*ESRF, 6 Rue Jules Horowitz, BP-220, 38043 Grenoble Cedex, France*

(Received 28 March 2013; accepted 10 June 2013; published online 11 July 2013)

High energy synchrotron XRD was employed to determine the lattice strain $\varepsilon\{111\}$ and diffraction peak intensity ratio R{200} in tetragonal PZT ceramics, both in the virgin poled state and after a bipolar fatigue experiment. It was shown that the occurrence of microstructural damage during fatigue was accompanied by a reduction in the gradient of the $\varepsilon\{111\}$–$\cos^2\psi$ plot, indicating a reduction in the level of residual stress due to poling. In contrast, the fraction of oriented 90° ferroelectric domains, quantified in terms of R{200}, was not affected significantly by fatigue. The change in residual stress due to fatigue is interpreted in terms of a change in the average elastic stiffness of the polycrystalline matrix due to the presence of inter-granular microcracks.
 [http://dx.doi.org/10.1063/1.4812326]

I. BACKGROUND

Fatigue processes in ferroelectric ceramics have been discussed for many years in relation to the use of such materials in piezoelectric actuators and ferroelectric memories.[1–3] In this context, the term *fatigue* is usually employed to describe changes in the functional properties over time as a result of static or alternating electrical and mechanical loads. On the other hand, the term *ageing* normally refers to a time-dependent decay of the dielectric and piezoelectric properties in the absence of any external stimulus.[4]

Several different mechanisms have been identified as the origin of fatigue in ferroelectrics; these include microcrack growth and coalescence due to internal residual stresses,[5,6] space charge formation,[2] and point defect clustering.[7–9] The development of fatigue depends on a variety of factors such as the nature of the load (electrical, mechanical),[9,10] type of waveform (unipolar, bipolar, sesquipolar),[11,12] frequency,[13] the chemical composition and structure/microstructure of the material,[14] and other environmental factors such as temperature.[15,16] Fatigue damage may also be localized in the near-electrode regions.[17,18] This combination of factors has led to some complexity in the interpretation of fatigue phenomena and means that it is difficult to draw general conclusions concerning the relative importance of the different mechanisms for a given material or device type.

The focus of the present study is on fatigue induced by fluctuations in residual inter-granular stress in polycrystalline PZT (lead zirconate titanate) ceramics. Such materials still represent the dominant type of piezoceramic in commercial applications, although lead-free compositions are being actively developed. Recent research on lead-free piezoceramics suggests that the mechanisms responsible for fatigue are similar to those observed in PZT ceramics; therefore, an improved understanding of fatigue phenomena in PZT ceramics should also be beneficial for lead free piezoelectrics such as those based on sodium potassium niobate and sodium bismuth titanate.[19]

The present authors have proposed a micromechanical model to describe the development of residual stress due to domain switching in polycrystalline ferroelectrics, using an approach based on the classical Eshelby inclusion method.[20–22] The model is supported by experimental measurements of the changes in ferroelectric domain orientations and crystal lattice strain as a function of the grain orientation, ψ, relative to the electric field direction, obtained using high energy synchrotron XRD (X-ray diffraction). The observed lattice strain under an applied electric field is a sum of two contributions, which are the intrinsic piezoelectric effect and the elastic strain caused by residual inter-granular stress;[23] the latter contribution is a result of the misfit, or eigenstrain, between a grain and the surrounding polycrystalline matrix, which undergoes an average transformation strain due to ferroelectric domain switching.

The identification of residual stress as a significant extrinsic contributor to lattice strain is an important breakthrough, since it was mistakenly assumed in some earlier publications that the observed lattice strain was due solely to the intrinsic piezoelectric effect.[24,25] This view has been confirmed by recent studies, in which the intrinsic and extrinsic contributions to the macroscopic strain of PZT ceramics in the sub-coercive field region were quantified using a combination of XRD and macroscopic property measurements.[26,27]

The purpose of the present study is to evaluate the changes in residual stress caused by fatigue in tetragonal PZT ceramics using high energy synchrotron XRD. The use of high energy x-rays, with the diffraction patterns being recorded in transmission, ensures that the true bulk behavior is obtained, in contrast to the near-surface region that is probed using conventional laboratory x-ray diffractometers. The degree of ferroelectric domain switching is quantified in

[a)]Author to whom correspondence should be addressed. Electronic mail: David.A.Hall@manchester.ac.uk

terms of the ratio of the (002) diffraction peak intensity to the sum of the (200) and (002) peak intensities, while the elastic strain is obtained from the position of the {111} diffraction peak. It was noted previously that the component of ferroelectric domain switching strain along ⟨111⟩ is zero in tetragonally distorted perovskite ferroelectrics and therefore, the {111} plane spacing serves as a sensor for lattice elastic strain in the remanent poled state (i.e., in the absence of an applied electric field). The influence of temperature on the fatigue behavior is also assessed in terms of its effect on the tetragonality, or c/a ratio, of the material.

II. EXPERIMENTAL METHODS

Specimens of a commercial hard PZT ceramic, type Ferroperm^{TM} Pz26, were provided by Meggitt in the form of disks having a thickness of 1 mm and diameter 10 mm. This material is prepared by a conventional solid-state synthesis process and the crystal structure is tetragonal, the composition being close to the morphotropic phase boundary. The average grain size in the sintered ceramic is approximately 8 μm as determined by a linear intercept method.

Fatigue tests were performed by applying a continuous sinusoidal bipolar electric field waveform with an electric field amplitude of 4 MV m^{-1}, the test specimen being contained in a temperature-controlled silicone oil bath. A relatively low frequency of 2 Hz was employed in order to avoid internal heating effects due to the hysteresis loss. Test signals representing the applied voltage and induced current were monitored continuously using a PC with a 16-bit A/D card. Numerical integration of the current waveform yielded the polarization, enabling the P-E hysteresis loops to be recorded at selected times during the experiment.

Rectangular beam-shaped specimens having dimensions of 1 mm × 1 mm × 3 mm were cut from the fatigued disks by diamond machining. Microstructural examination was carried out on polished specimens, using a Philips 525 SEM. High energy synchrotron XRD was conducted at ESRF (European Synchrotron Radiation Facility), Grenoble, France, using an X-ray wavelength of 0.153572×10^{-10} m. The use of high energy X-rays (80.7 keV) gives ~30% transmission through the sample, despite the highly absorbing material. Diffraction patterns were obtained in transmission using a Frelon 2-D detector and with a specimen to camera distance of approximately 1 m. The conversion to 1-D diffraction patterns was carried out using the Fit2D software package.[28] The 2-D image data, which covered just over a quarter of the circular diffraction pattern, were caked into ten 1-D slices with Fit2D, yielding 1-D diffraction patterns covering grain orientations from 0 to 90° ψ (azimuthal orientation). Peak profiles were then fitted using X-fit.[29]

The lattice strain $\varepsilon\{111\}$ was obtained by determining the change in the {111} lattice spacing relative to the unstressed value, $d_0\{111\}$. The value of $d_0\{111\}$ was itself determined by plotting $d\{111\}$ as a function of $\cos^2\psi$ and calculating the value of $d\{111\}$ for which $\cos^2\psi = 1/3$. This method is based on the identification of the zero strain condition for a ferroelectric ceramic in the remanent poled state.[20] The preferred orientation due to ferroelectric domain switching was quantified in terms of the ratio of the diffraction peak intensities, $I_{(002)}$ and $I_{(200)}$, expressed as

$$R\{200\} = \frac{I_{(002)}}{I_{(002)} + I_{(200)}}. \quad (1)$$

In the present results, the value of $R\{200\}$ at $\cos^2\psi = 1/3$ was determined as 0.32, which indicates that the structure factors for the (200) and (002) reflections are similar, and therefore, the value of $R\{200\}$ is approximately equal to the fraction of *c*-axis oriented domains.

High temperature XRD measurements were obtained from an unpoled disk-shaped specimen, during heating from 30 to 400 °C. A PANalytical MPD diffractometer was used in conjunction with an Anton Paar HTK1200 oven. Data were collected in the range of 2θ from 20 to 60°, in steps of ~0.033° for a total time of 1 h per temperature. The sample was heated at a rate of 5 °C per minute, allowing 5 min to reach equilibrium prior to measurement. Programmable divergence slits were used in order to minimize air scattering at low angles and improve statistics at high angles.

III. RESULTS AND DISCUSSION

A. Ferroelectric hysteresis measurements

Representative P-E hysteresis loops, obtained during the fatigue test at 30 °C, are illustrated in Fig. 1. The initial loop, at t = 0 s, was relatively narrow and exhibited low remanent, P_r, and maximum, P_{max}, polarization values of 0.15 and 0.24 C m^{-2}, respectively. The appearance of this initial loop is typical for a hard, acceptor-doped ferroelectric ceramic after ageing for some time in the unpoled state. The reorientation of acceptor ion-oxygen vacancy dipolar defects towards the local domain polarization tends to restrict domain wall motion, leading to a reduction of the switchable polarization.[30] A field-forced *deageing* effect was observed during the first 12 000 s of the fatigue test, characterized by gradual increases in the polarization and coercive electric field values over time. This effect has been explained previously in terms of a time-dependent randomization of the dipolar defect orientations under the influence of the alternating electric field, which reduces their influence on ferroelectric domain switching.[31,32] At later times, the P_r and P_{max} values reduced significantly while the coercive field, E_c, continued to increase, due to the onset of fatigue, as shown in Fig. 1(b).

The changes in the polarization and coercive field values during the fatigue test are summarized in Fig. 2, which also includes the data for a test carried out at a temperature of 90 °C for comparison. The peak value of P_r occurred after approximately 12 000 s at 30 °C, which indicates that the field-forced deageing effect was dominant up to this time. In contrast, only 3300 s was required to reach the peak polarization value at 90 °C. The influence of temperature on the deageing and ageing behaviour of hard ferroelectrics can be understood in terms of its effect on the activation energy for dipole reorientation.[29] An additional effect of the increase in temperature to 90 °C was that P_r decreased only slightly after reaching its peak value, while the rate of increase of E_c reduced at the same time. The latter observations indicate

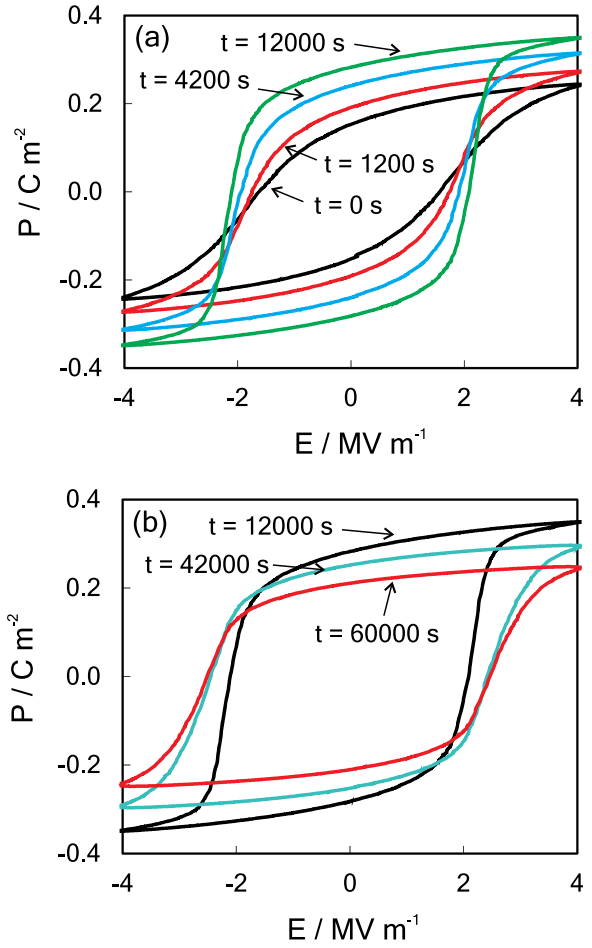

FIG. 1. Change in P-E Loops during the fatigue process at 30 °C (a) 0 to 12 000 s and (b) 12 000 to 60 000 s.

that the degradation in properties caused by fatigue was less pronounced at the higher temperature.

B. Microstructure

Examination of the microstructure by SEM revealed that the alternating electric field caused the initiation and propagation of intergranular microcracks, leading to the occurrence of some severely damaged regions distributed throughout the bulk of the specimen, as illustrated in Fig. 3. The presence of these microcracks means that there are regions in the specimen within which the inter-granular constraint is reduced or even completely absent. Therefore, it was anticipated that this should lead to a reduction in the average level of residual stress in the poled ceramic after the fatigue experiment.

C. Preferred domain orientation and lattice strain

Selected regions of the diffraction patterns for the poled PZT ceramic, obtained using high energy XRD, are presented in Fig. 4. The appearance of a single {111} reflection and a split (002)/(200) peak is typical for a tetragonally distorted perovskite ferroelectric. Comparing the position of the {111} peak for different grain orientations, it is evident that there was a shift to lower scattering angles as ψ varied from 90° to 0°. This indicates that the {111} lattice spacing is

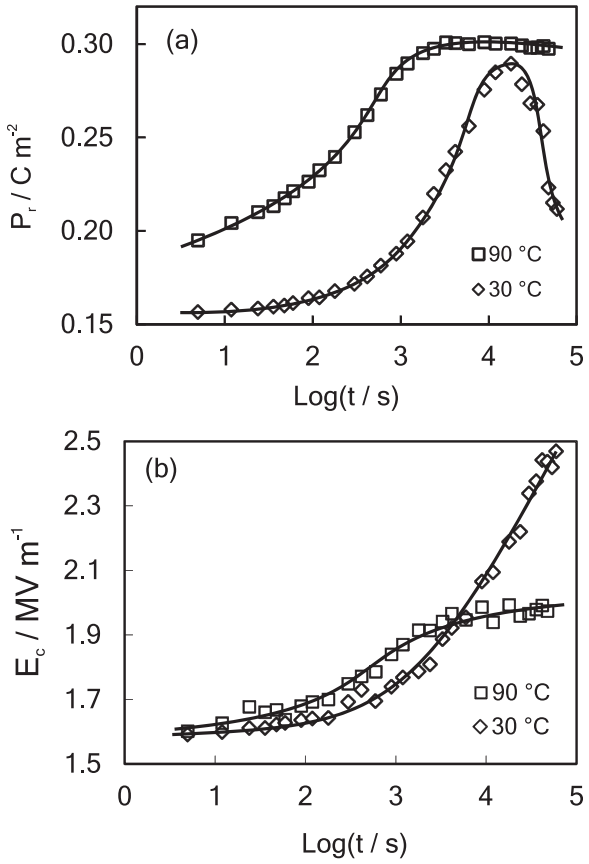

FIG. 2. Changes in (a) P_r and (b) E_c during the fatigue process.

subject to a tensile strain for $\psi = 0°$ and a compressive strain for $\psi = 90°$. The {200} diffraction peaks, presented in Fig. 4(b), show changes in intensity that indicate a preference for *c*-axis (002)-oriented domains for $\psi = 0°$, and *a*-axis (200) or (020)-oriented domains for $\psi = 90°$. These variations in intensity provide the means to quantify the changes in 90° domain orientation caused by poling.

The $\varepsilon\{111\}$-$\cos^2\psi$ plot for the poled PZT ceramic, presented in Fig. 5(a), exhibits a linear relationship with a positive slope, confirming that the {111}-oriented grains experience tensile residual stress along the poling axis and

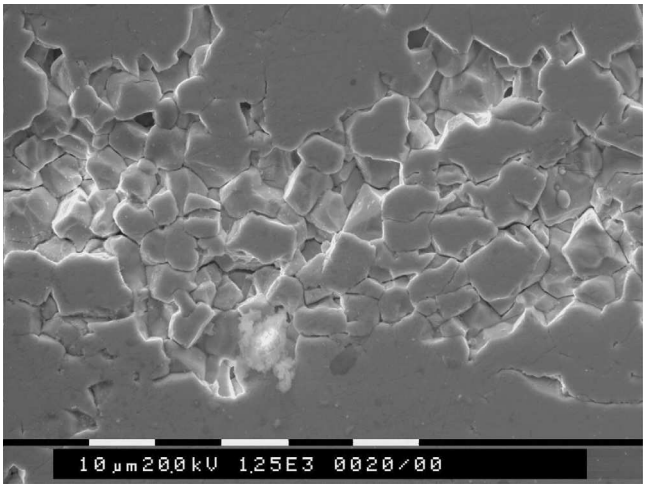

FIG. 3. SEM micrograph of specimen after fatigue for 60 000 s at 30 °C, showing evidence of microcracks and grain pull-out in a damaged region.

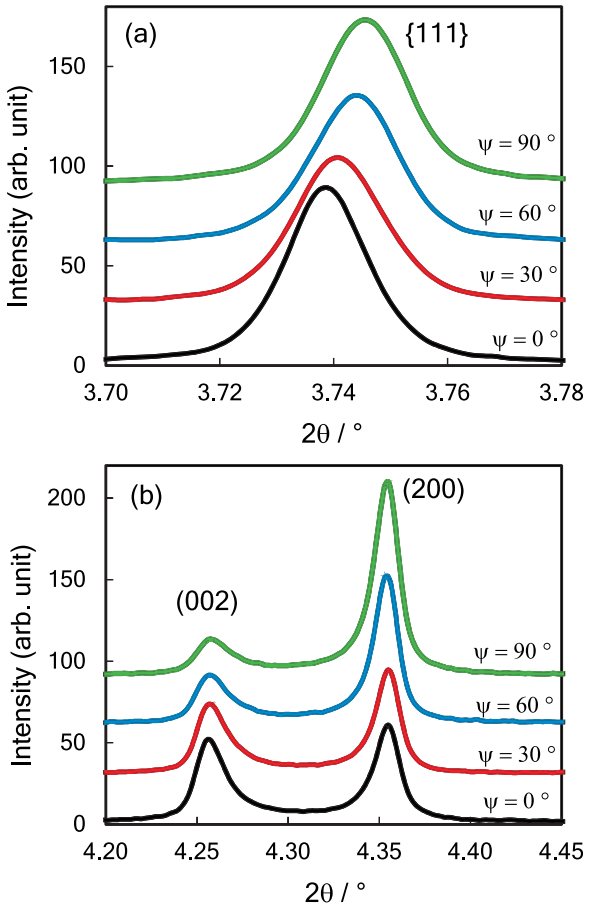

FIG. 4. XRD patterns for poled tetragonal PZT ceramic showing changes in position and intensity of (a) {111} and (b) {200} diffraction peaks for various grain orientations, ψ, relative to the electric field direction.

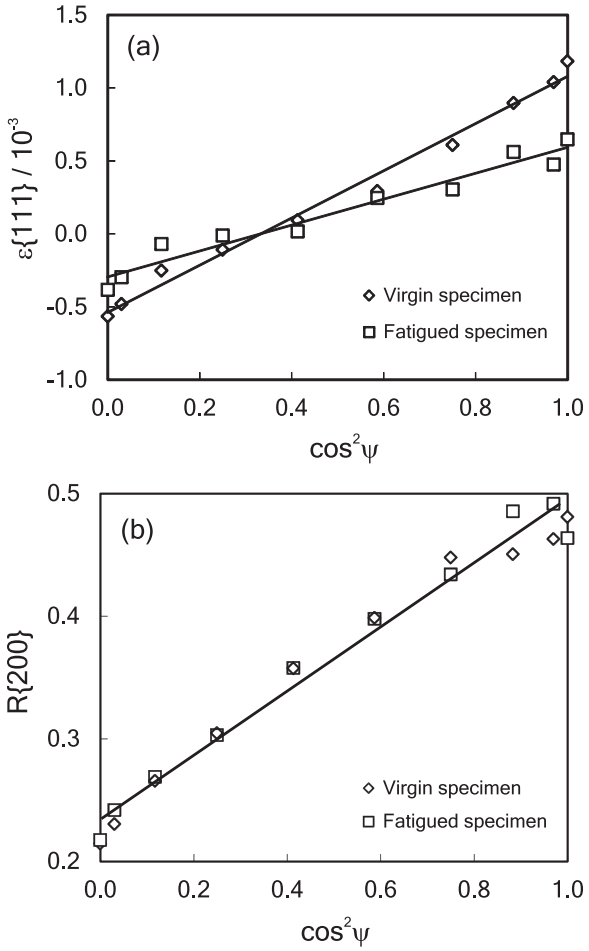

FIG. 5. Changes in (a) lattice strain $\varepsilon\{111\}$ and (b) peak intensity ratio R{200} as a function of grain orientation ψ, for virgin and fatigued specimens.

compressive residual stress in the orthogonal directions. The degree of preferred 90° domain orientation is presented in Fig. 5(b) in terms of the intensity ratio R{200}, which also shows an approximately linear dependence on $\cos^2\psi$. The correlation between $\varepsilon\{111\}$ and R{200} was explained previously on the basis that each grain experiences an elastic misfit strain along $\langle 111\rangle$ caused by residual stress due to ferroelectric domain switching in the surrounding grains. Cyclic changes in residual stress due to ferroelectric domain switching under the influence of the alternating bipolar electric field are responsible for the initiation and propagation of microcracks, which appear to be the dominant fatigue mechanism for this type of tetragonal PZT ceramic under these specific loading conditions.

The slope of the $\varepsilon\{111\}$-$\cos^2\psi$ plot for the specimen subjected to the fatigue test at 30 °C was significantly lower than that of the virgin poled specimen, suggesting that the average level of residual stress was affected strongly by the fatigue process. For example, the maximum strain at $\cos^2\psi = 1$ was 1.09×10^{-3} for the virgin poled specimen and 0.59×10^{-3} for the fatigued specimen. The reduction in residual stress due to fatigue can be explained by a reduction in the level of inter-granular constraint due to the development of the microcracked regions, as discussed further below.

In contrast to the case of lattice strain, the slope of the R{200}-$\cos^2\psi$ plot was not affected significantly by fatigue, indicating that the degree of preferred 90° domain orientation at zero electric field did not change during the latter part of the fatigue test. This observation appears to contradict the results of the P-E measurements during the fatigue test (Fig. 2), which showed a sharp reduction in P_r after fatigue for 12 000 s. It is likely that this is due to local electric field screening by microcracks so that some grains, although initially polarized in the positive or negative directions, experience a local electric field strength that is less than E_c and, therefore, are unable to contribute to the switchable polarization. The continuous increase in the macroscopic E_c value during the fatigue test provides further evidence to support this view.

The magnitude of the residual stress, and therefore the driving force for crack propagation, is dependent on the transformation strain due to ferroelectric domain switching, which in turn is related to the tetragonality ratio, c/a. Using the laboratory X-ray diffractometer, it was found that the c/a ratio for the tetragonal PZT ceramic decreased from 1.023 at 30 °C to 1.020 at 90 °C, as shown in Fig. 6. Although these results demonstrate a relatively small reduction in tetragonality on heating, it could still be sufficient to explain the observed changes in fatigue behavior at elevated temperatures.[16]

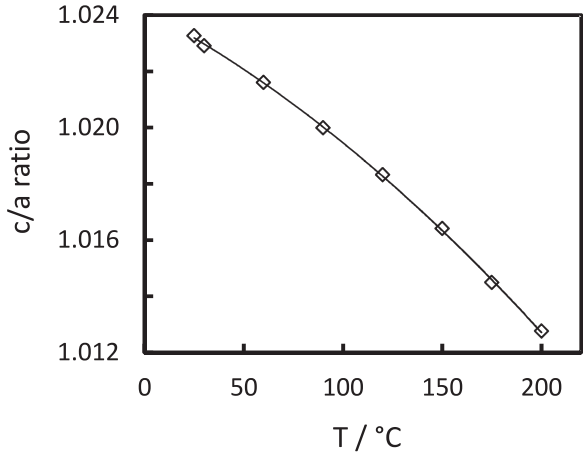

FIG. 6. Variation of c/a ratio for tetragonal PZT ceramic as a function of temperature.

D. Estimate of stiffness in fatigued state

A first order approach is presented here in order to explain the reduction of residual stress during fatigue in terms of a decrease in the average stiffness of the polycrystalline ceramic. This reduction in stiffness is a direct result of the microstructural damage. It is apparent that the average domain switching strain is the same in the virgin and fatigued states as is evident in the data presented in Fig. 5(b). We further assume that a grain, approximated as a spherical inclusion, is subjected to an electric field along the X_3-direction of the specimen, referenced to conventional Cartesian axes.

After poling and removal of the electric field, the specimen has an average macroscopic strain due to ferroelectric domain switching, ε^0, which has the components

$$\varepsilon^0 = \begin{pmatrix} -\bar{\varepsilon}/2 & 0 & 0 \\ 0 & -\bar{\varepsilon}/2 & 0 \\ 0 & 0 & \bar{\varepsilon} \end{pmatrix}, \tag{2}$$

where $\bar{\varepsilon}$ is the axial component of the macroscopic strain along the X_3-axis. The difference between the poling strain (transformation strain) of the grain under consideration, ε^P, and the macroscopic strain, ε^0, is the eigenstrain, or misfit strain, ε^*, assigned to the grain

$$\varepsilon^* = \varepsilon^P - \varepsilon^0. \tag{3}$$

For a $\langle 111 \rangle$ oriented grain, the transformation strain due to domain switching is zero, as noted previously, and therefore the eigenstrain, ε^* is

$$\varepsilon^* = \begin{pmatrix} \bar{\varepsilon}/2 & 0 & 0 \\ 0 & \bar{\varepsilon}/2 & 0 \\ 0 & 0 & -\bar{\varepsilon} \end{pmatrix}. \tag{4}$$

We consider that the elastic stiffness C of the grain itself is not affected by the fatigue process, since cracking occurs along grain boundaries. However, the average stiffness of the polycrystalline matrix surrounding the grain is changed to $\bar{C}$ as a result of the microcracking.

The elastic stress, σ, of the grain is evaluated by first solving the equivalent condition[33]

$$\sigma = \bar{C}(S\varepsilon^{**} - \varepsilon^{**}) = C(S\varepsilon^{**} - \varepsilon^*). \tag{5}$$

Here, S is the Eshelby tensor,[34] which is assumed to be the same in the virgin and fatigued states. ε^{**} is the eigenstrain of an equivalent inclusion that has elastic stiffness $\bar{C}$ and reproduces the total strain and stress due to the actual eigenstrain of ε^*. In Eq. (5), $S\varepsilon^{**}$ represents the total strain (constraint strain) in both the actual and equivalent inclusions.

Rearranging Eq. (5) yields

$$\varepsilon^{**} = \{\bar{C} + (C - \bar{C})S)\}^{-1} C\varepsilon^*). \tag{6}$$

The elastic strain in the grain, ε, is calculated from

$$\varepsilon = S\varepsilon^{**} - \varepsilon^*. \tag{7}$$

Using Eqs. (6) and (7), we can evaluate the ratio of the elastic strain in the fatigued state to that in the virgin state. In this evaluation, $\bar{C}$ is assumed to be αC, where $0 \leq \alpha \leq 1$.

It was assumed in the calculation that $C_{11} = 153$ GPa, $C_{12} = 103$ GPa. A Poisson ratio of $\nu = 0.39$ was obtained from these values. The approximate isotropic stiffness values, C_{11} and C_{12}, were obtained by averaging over the anisotropic stiffness values provided by the manufacturer.

The Eshelby tensors employed in the calculation are expressed in terms of the Poisson ratio, as follows:[34]

$$S_{1111} = \frac{7 - 5\nu}{15(1 - \nu)}, \tag{8}$$

$$S_{1122} = \frac{5\nu - 1}{15(1 - \nu)}. \tag{9}$$

The results of an example calculation to show the relationship between the elastic strain ratio, R_ε, and the stiffness ratio, α, are illustrated in Fig. 7. According to this calculation, the observed elastic strain ratio of 0.54 for the fatigued specimen corresponds to a stiffness ratio of approximately 0.38. Although many simplifying assumptions are involved in the above calculation, it provides a useful first-order estimate of the change in stiffness due to fatigue.

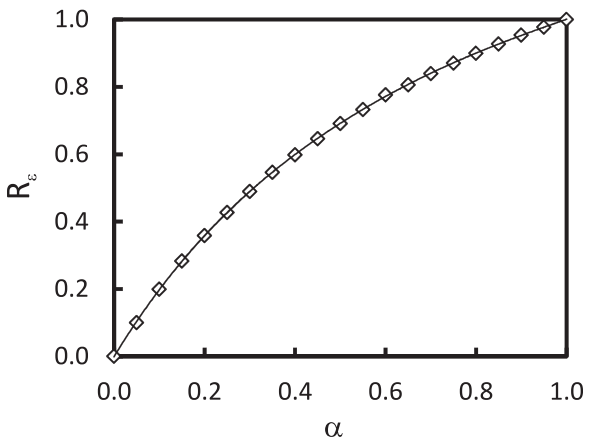

FIG. 7. Calculated relationship between $\langle 111 \rangle$ lattice strain ratio, R_ε, and Young's modulus ratio, α.

From Eqs. (5) and (7), the stress in the grain is calculated as

$$\sigma = C(S\varepsilon^{**} - \varepsilon^{*}). \tag{10}$$

We can also estimate the elastic strain and stress in the following manner. In the virgin state ($\alpha = 1$), the measured elastic strain is 1.09×10^{-3} along the poling direction. For this value of elastic strain, the macroscopic strain along the poling direction, $\bar{\varepsilon}$, is calculated as 1.98×10^{-3} from Eq. (7). This result is in reasonable agreement with that determined previously for a soft tetragonal PZT ceramic.[21] Similarly, for the fatigued specimen ($\alpha = 0.38$) the elastic strain along the poling direction is 0.59×10^{-3}. We assume that the macroscopic poling strain remains the same in the virgin and fatigued states, since the R{200} values were similar, as shown in Fig. 5(b). With these assumptions, the corresponding stresses in the virgin and fatigued states are calculated as 55 MPa and 31 MPa, respectively.

IV. CONCLUSIONS

It has been demonstrated that high energy synchrotron XRD can be used to quantify changes in residual stress due to bipolar fatigue in PZT ceramics. The lattice elastic strain $\varepsilon\{111\}$ was reduced from 1.09×10^{-3} for a virgin poled specimen to 0.59×10^{-3} for a specimen subjected to a fatigue test at 30 °C, indicating a significant reduction in the residual stress associated with the poled state. Microstructural examination of the fatigued specimen revealed that the fatigue damage occurred in the form of localized inter-granular microcracking, which occurred as a result of the cyclic changes in residual stress caused by large-scale ferroelectric domain switching. The reduction in residual stress due to fatigue could be described adequately in terms of a reduction in the average elastic stiffness of the polycrystalline matrix, although a more accurate model should also include consideration of the anisotropic elastic properties of poled ferroelectric ceramics and the heterogeneous distribution of the fatigue damage.

ACKNOWLEDGMENTS

The authors wish to thank ESRF for provision of synchrotron radiation facilities.

[1]K. Uchino, Acta Mater. **46**, 3745 (1998).
[2]W. L. Warren, J. Appl. Phys. **77**, 6695 (1995).
[3]D. C. Lupascu and J. Rödel, Adv. Eng. Mater. **7**, 882 (2005).
[4]D. C. Lupascu, Y. A. Genenko, and N. Balke, J. Am. Ceram. Soc. **89**, 224 (2006).
[5]S. L. dos Santos e Lucato, D. V. Lupascu, M. Kamlah, J. Rödel, and C. S. Lynch, Acta Mater. **49**, 2751 (2001).
[6]J. Nuffer, D. C. Lupascu, A. Glazounov, H.-J. Kleebe, and J. Rödel, J. Eur. Ceram. Soc. **22**, 2133 (2002).
[7]M. Dawber and J. F. Scott, Appl. Phys. Lett. **76**, 1060 (2000).
[8]J. F. Scott and M. Dawber, Appl. Phys. Lett. **76**, 3801 (2000).
[9]J. Nuffer, D. C. Lupascu, and J. Rödel, Acta Mater. **48**, 3783 (2000).
[10]D. C. Lupascu, E. Aulbach, and J. Rödel, J. Appl. Phys. **93**, 5551 (2003).
[11]N. Balke, D. C. Lupascu, T. Granzow, and J. Rödel, J. Am. Ceram. Soc. **90**, 1081 (2007).
[12]N. Balke, D. C. Lupascu, T. Granzow, and J. Rödel, J. Am. Ceram. Soc. **90**, 1088 (2007).
[13]N. Zhang, L. Li, and Z. Gui, J. Eur. Ceram. Soc. **21**, 677 (2001).
[14]C. Verdier, F. D. Morrison, D. C. Lupascu, and J. F. Scott, J. Appl. Phys. **97**, 024107 (2005).
[15]J. Glaum, T. Granzow, L. A. Schmitt, H.-J. Kleebe, and J. Rödel, Acta Mater. **59**, 6083 (2011).
[16]D. Wang, Y. Fotinich, and G. P. Carman, J. Appl. Phys. **83**, 5342 (1998).
[17]N. Balke, D. C. Lupascu, T. Blair, and A. Gruverman, J. Appl. Phys. **100**, 114117 (2006).
[18]N. Balke, H. Kungl, T. Granzow, D. C. Lupascu, M. J. Hoffmann, and J. Rödel, J. Am. Ceram. Soc. **90**, 3869 (2007).
[19]Z. Luo, J. Glaum, T. Granzow, W. Jo, R. Dittmer, M. Hoffman, and J. Rödel, J. Am. Ceram. Soc. **94**, 529 (2011).
[20]D. A. Hall, A. Steuwer, B. Cherdhirunkorn, T. Mori, and P. J. Withers, J. Appl. Phys. **96**, 4245 (2004).
[21]D. A. Hall, A. Steuwer, B. Cherdhirunkorn, P. J. Withers, and T. Mori, J. Mech. Phys. Solids **53**, 249 (2005).
[22]D. A. Hall, A. Steuwer, B. Cherdhirunkorn, T. Mori, and P. J. Withers, Acta Mater. **54**, 3075 (2006).
[23]D. A. Hall, T. Mori, P. J. Withers, H. Kungl, M. J. Hoffmann, and J. Wright, Mater. Sci. Technol. **24**, 927 (2008).
[24]J.-T. Reszat, A. E. Glazounov, and M. J. Hoffmann, J. Eur. Ceram. Soc. **21**, 1349 (2001).
[25]R. Guo, L. E. Cross, S.-E. Park, B. Noheda, D. E. Cox, and G. Shirane, Phys. Rev. Lett. **84**, 5423 (2000).
[26]A. Pramanick, J. E. Daniels, and J. L. Jones, J. Am. Ceram. Soc. **92**, 2300 (2009).
[27]A. Pramanick, D. Damjanovic, J. E. Daniels, J. C. Nino, and J. L. Jones, J. Am. Ceram. Soc. **94**, 293 (2011).
[28]A. P. Hammersley, S. O. Svensson, M. Hanfland, A. N. Fitch, and D. Häusermann, High Press. Res. **14**, 235 (1996).
[29]A. A. Coelho and R. W. Cheary, X-FIT, CCP14 Library, http://www.ccp14.ac.uk, 1996.
[30]K. Carl and K. H. Härdtl, Ferroelectrics **17**, 473 (1977).
[31]R. Lohkämper, H. Neumann, and G. Arlt, J. Appl. Phys. **68**, 4220 (1990).
[32]U. Robels and G. Arlt, J. Appl. Phys. **73**, 3454 (1993).
[33]J. D. Eshelby, Proc. R. Soc. London, Ser. A **252**, 561 (1959).
[34]J. D. Eshelby, Proc. R. Soc. London, Ser. A **241**, 376 (1957).